Hindawi
Journal of Chemistry
Volume 2021, Article ID 3834368, 8 pages
https://doi.org/10.1155/2021/3834368

Research Article

Cocrystallization of Febuxostat with Pyridine Coformers: Crystal Structural and Physicochemical Properties Analysis

Lei Gao and Xianrui Zhang

College of Chemical Engineering and Resource Recycling, Wuzhou University, Wuzhou 543000, China

Correspondence should be addressed to Xianrui Zhang; zhangyang159246@163.com

Received 1 October 2021; Revised 27 November 2021; Accepted 30 November 2021; Published 16 December 2021

Academic Editor: Franc Perdih

Drug cocrystals and salts have promising applications for modulating the physicochemical properties and solubility of pharmaceuticals. In this study, a cocrystal and two salts of febuxostat (FEB) with pyridine nitrogen coformers, including 4, 4′-bipyridine (BIP), 3-aminopyridine (3AP) and 4-hydroxypyridine (4HP), were designed to improve the solubility of FEB. The single-crystal structures were elucidated, and their physical and chemical properties were investigated by IR, PXRD, and DSC. In addition, drug-related properties, including the solubility and powder dissolution rate were assessed. The solubility and powder dissolution studies showed that the FEB-BIP cocrystal and FEB-3AP salt have superior dissolution compared to FEB.

1. Introduction

Over the past decades, drug cocrystals and salts screening has been an important tool for optimizing the drug-forming properties [1–8]. Due to the diversity of cocrystal formers (CCFs), researchers can design drug cocrystal and salt forms in a targeted manner to optimize their solubility, mechanical properties, hygroscopicity, stability, and bioavailability [9–14]. However, due to the low success rate of the screening process, it remains a challenge to rationally assemble the structure of API molecules through hydrogen bonding to obtain the desired properties in drug crystal engineering. Thus, cocrystal and salt screening has become an essential part of the preliminary drug development process [15].

Febuxostat (2-(3-cyano-4-isobutoxyphenyl)-4-methylthiazole-5-carboxylic acid, FEB) is a famous nonpurine selective inhibitor of xanthine oxidase for the treatment of gout [16–18]. FEB is classified as a biopharmaceutical classification system (BCS) II compound with a low water solubility and high penetrability. Its poor aqueous solubility affects its absorption in the body and limits its bioavailability. Many previous reports have shown that cocrystals and salts can improve the solubility of febuxostat [12, 19–24]. Herein, we designed new cocrystal or salt forms of febuxostat to modulate its solubility and dissolution rate. Based on the structural analysis of previous-reported cocrystals and salts of febuxostat, we identified those cocrystal coformers containing pyridine nitrogen with the potential to form hydrogen bonds with FEB. Thus, a series of cocrystal coformers containing pyridine nitrogen was employed to screen the cocrystals and salts of FEB (Supplementary Materials, Figure S1). The ΔpKa values between FEB and coformers are given in Table S1. For acid-base complex whose ΔpKa >3, the probability of salt formation will be high, and when 0 <ΔpKa <3, it is difficult to predict whether proton transfer will occur [14, 25, 26]. Whether the final product is a cocrystal or a salt will be disclosed by crystallographic data. The main research is focused on the crystallographic investigations of these novel crystalline samples. Finally, a novel cocrystal of FEB and 4, 4′-bipyridine (BIP) and two salts of 3-aminopyridine (3AP) and 4-hydroxypyridine (4HP) were successfully designed, synthesized, and characterized (Figure 1).

2. Materials and Methods

2.1. Materials and Equipment. All chemicals were obtained from commercial sources and were used as received. Fourier infrared (IR) spectra were performed on a Nicolet iS5 FTIR

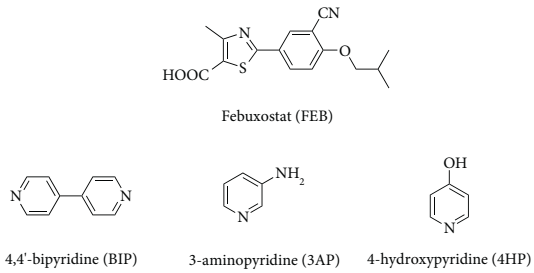

Figure 1: Chemical structures of FEB and coformers.

spectrometer in the scan range of 4000–400 cm^{-1} range. The thermal properties were measured on a Mettler-Toledo differential scanning calorimeter (DSC) equipped with a heating rate of 10°C/min using N_2 as the dry air. Powder X-ray diffraction (PXRD) measurements were collected using a German Bruker corporation D8 ADVANCE X-ray diffractometer. All single-crystal X-ray diffraction data were recorded on a Bruker Apex-II CCD diffractometer with enhanced Mo-Kα radiation ($\lambda = 0.71073$ Å). All crystal structures were determined by direct methods using the SHELXS program and refined by the SHELXL program package [27]. Crystallographic data of the FEB cocrystal and salts are given in Table 1, and the hydrogen bond parameters are given in Table 2.

2.2. Preparation of Cocrystal and Salts of FEB. Preparation of FEB-BIP (2 : 1) cocrystal: febuxostat (20.00 mg, 0.0632 mmol) and 4, 4′-bipyridine (9.87 mg, 0.0632 mmol) were dissolved in methanol (4 mL) or acetone (4 mL) at room temperature. Then, the solutions were allowed to evaporate slowly at room temperature for 4–6 days to obtain block crystals of FEB-BIP. A large amount of FEB-BIP samples were prepared by the solvent-assisted grinding. In a typical experiment, FEB (200 mg) and BIP (49.35 mg) were placed into an agate mortar and the obtained was ground three times with methanol (1 mL) to produce FEB-BIP.

Preparation of FEB-3AP (2 : 1) salt: febuxostat (20.00 mg, 0.0632 mmol) and 3AP (5.95 mg, 0.0632 mmol) were dissolved in acetonitrile (5 mL) at room temperature, and then, the solutions were allowed to evaporate slowly at room temperature for 5–8 days to obtain block crystals of FEB-3AP. A large amount of FEB-3AP samples were prepared by the solvent-assisted grinding. In a typical experiment, FEB (200 mg) and 3AP (29.75 mg) were placed into an agate mortar and the obtained was ground three times with acetonitrile (1 mL) to produce FEB-3AP.

Preparation of FEB-4HP-H_2O (1 : 1 : 1) salt: febuxostat (20.00 mg, 0.0632 mmol) and 4HP (6.01 mg, 0.0632 mmol) were dissolved in 5 mL of acetonitrile, and then, 100 μL of water was added into this solution. The solutions were allowed to evaporate slowly at room temperature for 5–8 days to get block crystals of FEB-4HP-H_2O. A large amount of FEB-4HP-H_2O samples were prepared by the solvent-assisted grinding. In a typical experiment, FEB (200 mg) and 4HP (60.1 mg) were placed into an agate mortar and the obtained was ground three times with the acetonitrile-water solvent mixture (49 : 1 v/v, 1 mL) to produce FEB-4HP-H_2O.

2.3. Solubility and Powder Dissolution Study. The equilibrium solubility tests were performed with a Shimadzu UV-2600 using the Beer–Lambert law at 315 nm. The concentrations of solubility and dissolution rate of the four samples (including FEB, FEB-BIP, FEB-3AP, and FEB-4HP-H_2O) were determined by a UV spectrophotometer, and the corresponding standard curve equations are given in Table S2. The solubility and powder dissolution were investigated by dissolving excess solid samples in water under a rotation speed of 500 rpm at 37°C. Approximately 100 mg FEB samples (or its cocrystal/salts) were deposited in a round-bottomed flask with a stopper containing 20 mL aqueous medium, followed by heating and stirring at a constant temperature of 37°C in a waterbath for 24 h. The solution was allowed to stand for 10 minutes, and then, the supernatant was removed and filtered through a 0.22 μm filter membrane. Then, the concentration was analyzed by UV after suitable dilution. The powder dissolution experiments were performed at 5, 10, 15, 20, 25, 30, 45, 60, 90, and 120 min and analyzed by UV.

3. Results and Discussion

3.1. Single-Crystal Structures. FEB-BIP cocrystal. The asymmetric unit of the FEB-BIP cocrystal contains one febuxostat molecule and one half of a 4, 4′-bipyridine molecule. In the cocrystal, two febuxostat molecules are connected by O2–H1···N3 (distance of 2.586 Å) hydrogen bonds to form a parallel chain (Figure 2). The parallel chains are held together via C18–H18···N2 (distance of 3.515 Å) and C20–H20···N2 (distance of 3.633 Å) hydrogen bonds to produce a two-dimensional sheet framework (Figure 3).

FEB-3AP salt: the asymmetric unit of the FEB-3AP salt contains one febuxostat molecule, one febuxostat anion, and one 3-aminopyridine cation caused by the proton transfer from the carboxylic acid of one febuxostat molecule to the pyridine ring of 3-aminopyridine. In the salt, one FEB anion and one 3AP cation are connected by $N6^{+}$-H6···$O2^{-}$ (distance of 2.660 Å) hydrogen bonds, and the other FEB molecule through O4–H1···O1 (distance of 2.471 Å) form intramolecular hydrogen bonds with the FEB anion (Figure 4). The trimers interacted with each other through N5–H5B···O5 (distance of 3.130 Å) hydrogen bonds to form zigzag chain structures (Figure 5).

FEB-4HP-H_2O salt: the crystal structure of FEB-4HP-H_2O salt was determined to be the triclinic P-1 space group. The Fourier maps show that the proton transfer and the generation of symmetric hydrogen bonds led to the formation of two complex dimers, including the FEB dimer anion and 4HP dimer cation (Supplementary Materials, Figure S2). In the salt, one FEB dimer anion is connected to one 4HP dimer cation by $N3^{+}$-H3···$O1^{-}$ (distance of 2.753 Å) hydrogen bonds to form a one-dimensional ribbon (Figure 6). The one-dimensional ribbons are extended by water molecules through O5–H5A···N1 and O5–H5B···O4 hydrogen bonding, forming a three-dimensional mesh structure. Moreover, the water molecules occupy the channels in the mesh structure (Figure 7).

Table 1: Crystallographic parameters of FEB cocrystal and salts.

Compounds	FEB-BIP (2 : 1)	FEB-3AP (2 : 1)	FEB-4HP-H_2O (1 : 1 : 1)
Empirical formula	$C_{21}H_{20}N_3O_3S$	$C_{37}H_{38}N_6O_6S_2$	$C_{21}H_{23}N_3O_5S$
Formula weight	394.46	726.85	429.48
Wavelength(A)	0.71073	0.71073	0.71073
Crystal system	Triclinic	Triclinic	Triclinic
Space group	*P*–1	*P*–1	*P*–1
a (Å)	9.1689 (5)	10.6113 (6)	8.9314 (7)
b (Å)	10.9904 (10)	12.1040(6)	8.9382 (8)
c (Å)	11.8036 (10)	15.3760 (7)	14.0069 (11)
α (°)	63.220 (9)	76.703 (4)	103.517 (7)
β (°)	79.983 (6)	81.454 (4)	98.686 (6)
γ (°)	89.499 (6)	70.809 (5)	99.661 (7)
V (Å^3)	1042.40 (14)	1809.40 (16)	1050.46 (16)
Z	2	2	2
T/K	293 (2)	293 (2)	293 (2)
Density (calculated) (g/cm^3)	1.257	1.334	1.358
Absorption coefficient (mm^{-1})	0.181	0.202	0.192
Parameters	260	482	278
F(000)	414	764	452
Goodness-of-fit on *F*2	1.013	1.021	1.014
Final *R* indices ($I > 2\sigma(I)$)	$R1 = 0.0554$ $\omega R2 = 0.1289$	$R1 = 0.0467$ $\omega R2 = 0.1084$	$R1 = 0.0769$ $\omega R2 = 0.1333$
$\Delta\rho$max/$\Delta\rho$min (e Å^{-3})	0.327/−0.233	0.254/−0.232	0.673/−0.578
CCDC	2002500	2099439	2099438

Table 2: Hydrogen bond parameters of FEB cocrystal and salts.

Compound	D-H···A	d (D-H)	d (H···A)	d (D···A)	<(DHA)	Symmetry code
FEB-BIP	O2–H1···N3	1.00	1.59	2.586 (3)	168	$x-1, y+1, z$
FEB-3AP	N5–H5B···O5	0.90	2.30	3.130 (3)	153	$-x+1, -y+1, -z$
	$N6^+$-H6···$O2^-$	1.00	1.68	2.660 (3)	164	$-x+2, -y+1, -z+1$
	O4–H1···O1	0.86	1.62	2.471 (3)	175	$x, y, z-1$
FEB-4HP-H_2O	$N3^+$-H3···$O1^-$	0.91	1.84	2.753 (4)	176	$x+1, y+1, z+1$
	O5–H5A···N1	0.85	2.21	2.983 (5)	150	$x+1, y+1$, z
	O5–H5B···O4	0.85	2.03	2.872 (5)	169	x, y, z

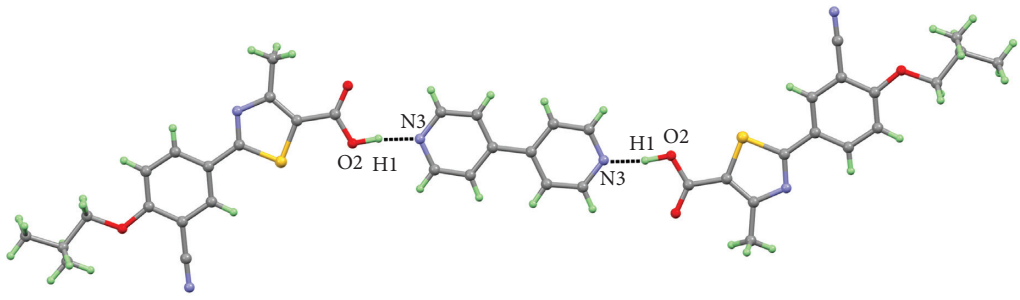

Figure 2: The parallel chain structures of FEB-BIP cocrystal.

3.2. PXRD Analysis. The experimental PXRD patterns of FEB-BIP, FEB-3AP, and FEB-4HP-H_2O were compared to FEB (Figure 8). This result showed that FEB-BIP, FEB-3AP, and FEB-4HP-H_2O exhibited significantly different characteristic peaks than that of FEB, which further confirms the formation of new crystalline forms. Moreover, the experimental PXRD patterns of FEB-BIP, FEB-3AP, and FEB-4HP-H_2O were in agreement with the corresponding single-crystal simulated data (Supplementary Materials, Figures S3–S5).

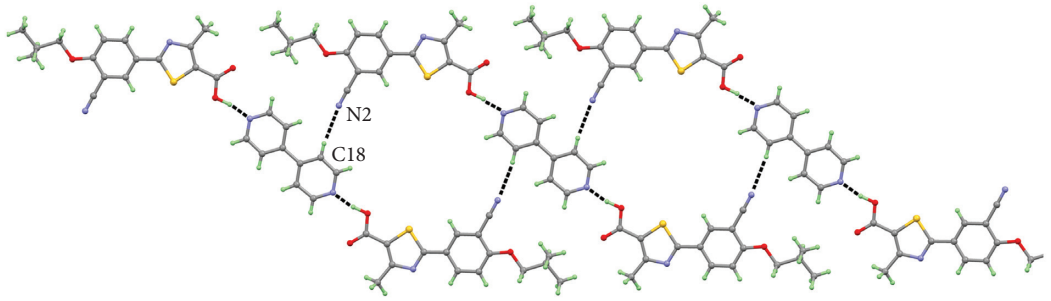

Figure 3: The two dimension sheet structures of FEB-BIP cocrystal.

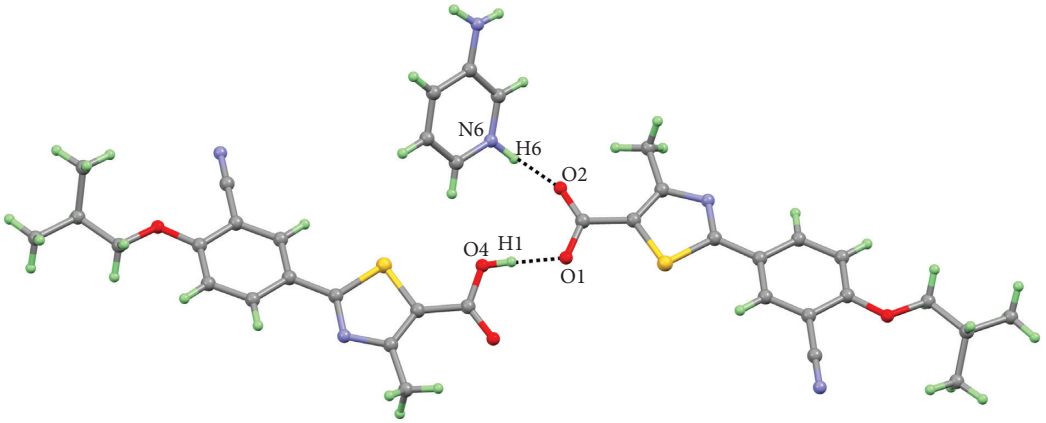

Figure 4: The crystal structures of FEB-3AP salt.

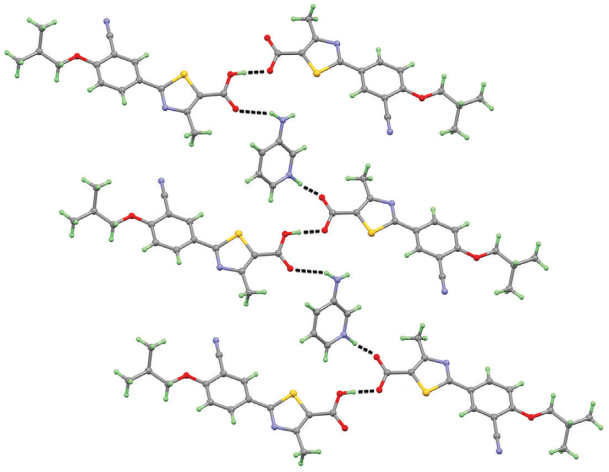

Figure 5: The zigzag chain structures of FEB-3AP salt.

3.3. IR Analysis. A comparative analysis of FTIR spectra for FEB, FEB-BIP, FEB-3AP, and FEB-4HP-H_2O is shown in Figure 9. FEB exhibits a characteristic peak at 1701 cm^{-1}, which is assigned to the C=O stretching vibration. FEB-BIP, FEB-3AP, and FEB-4HP-H_2O show the C=O stretching absorption peak at 1690, 1680, and 1699 cm^{-1}, respectively, which indicate the change of hydrogen bonding interactions on the asymmetric vCOO vibration.

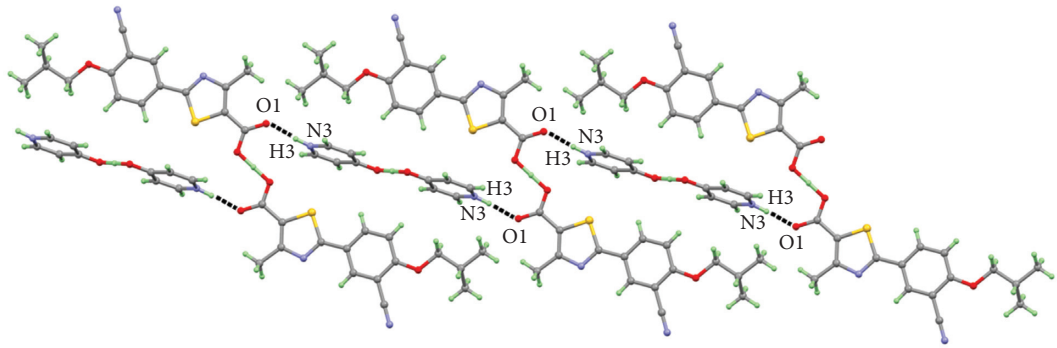

Figure 6: The crystal structures of FEB-4HP-H_2O salt.

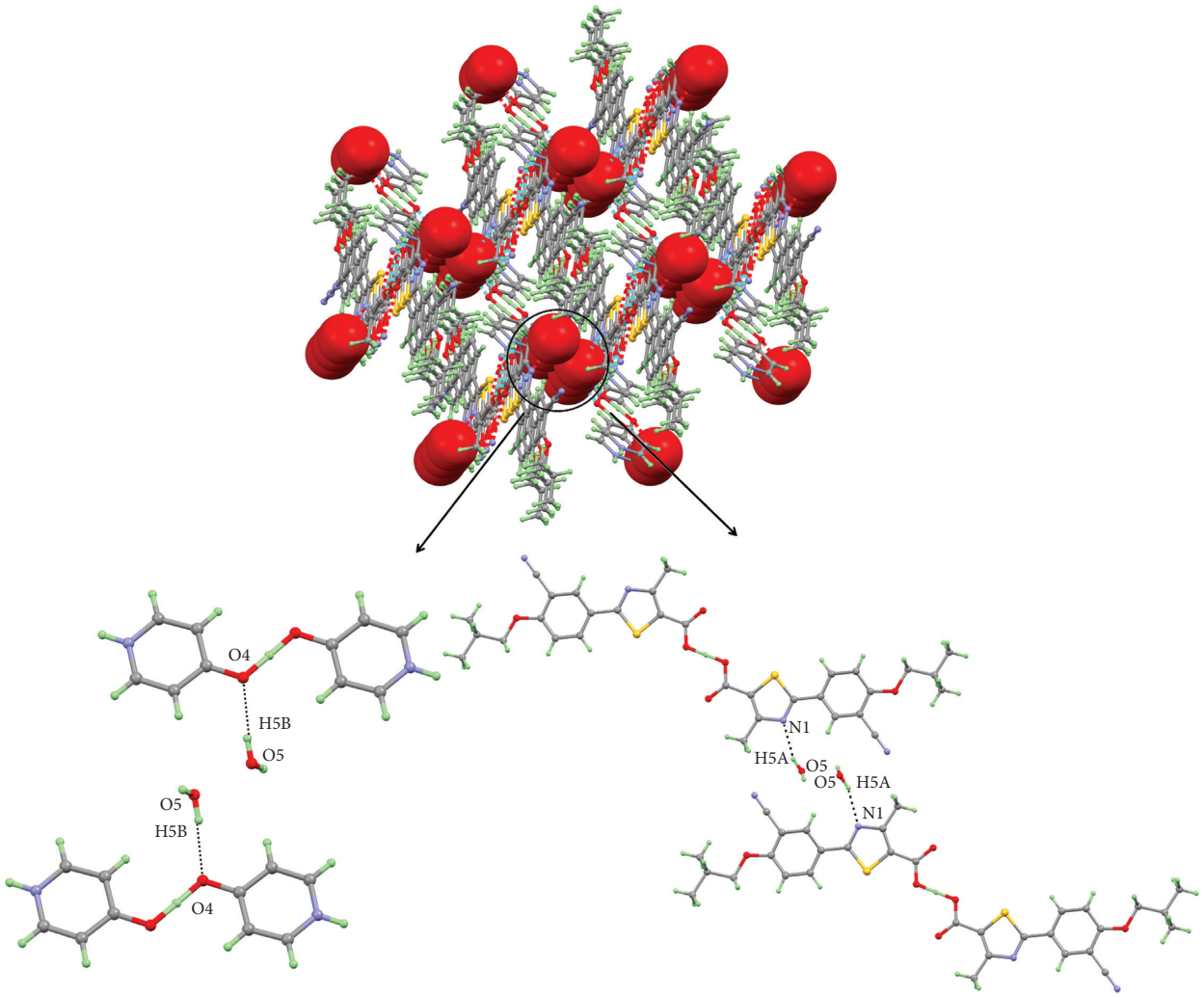

Figure 7: The visualization of water molecules in the crystal structure channel of FEB-4HP-H_2O salt.

3.4. DSC Analysis. The thermodynamic stability of FEB, FEB-BIP, FEB-3AP, and FEB-4HP-H_2O was examined by DSC (Figure 10), and they all exhibited single melting endothermic peaks at 201°C, 219°C, 186°C, and 151°C, respectively. Thus, the sequence of the thermodynamic stability is FEB-BIP > FEB > FEB-3AP > FEB-4HP-H_2O.

3.5. Solubility and Powder Dissolution Rate Analysis. Solubility is a thermodynamic property that directly affects the in vivo absorption of orally administered drugs. The solubility and powder dissolution of FEB, FEB-BIP cocrystal, FEB-3AP salt, and FEB-4HP-H_2O salt were determined in water at 37°C. The residual samples analysis showed that

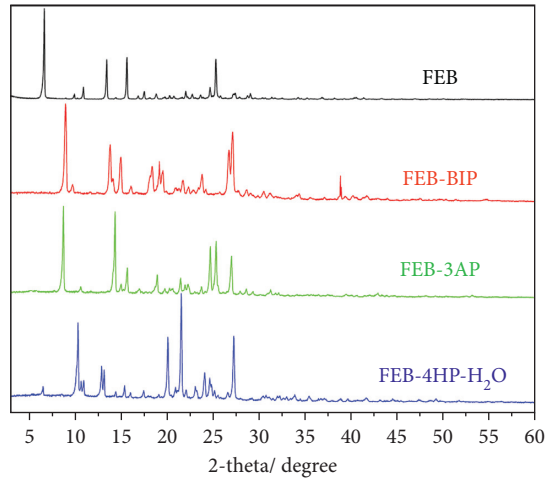

Figure 8: PXRD pattern of FEB (black), FEB-BIP cocrystal (red), FEB-3AP salt (green), and FEB-4HP-H_2O salt (blue).

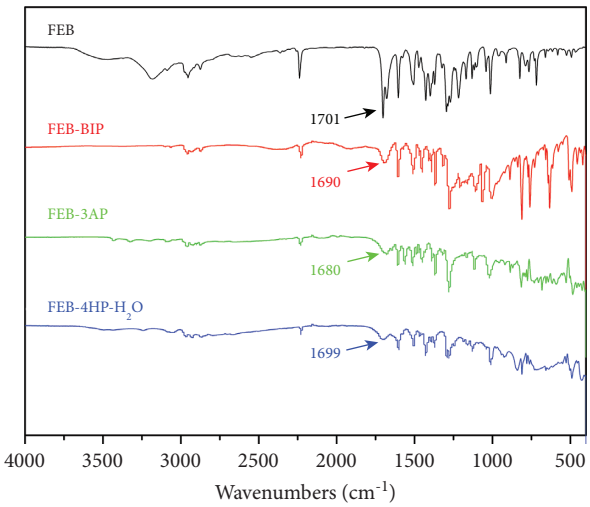

Figure 9: IR spectra of FEB (black), FEB-BIP cocrystal (red), FEB-3AP salt (green), and FEB-4HP-H2O salt (blue).

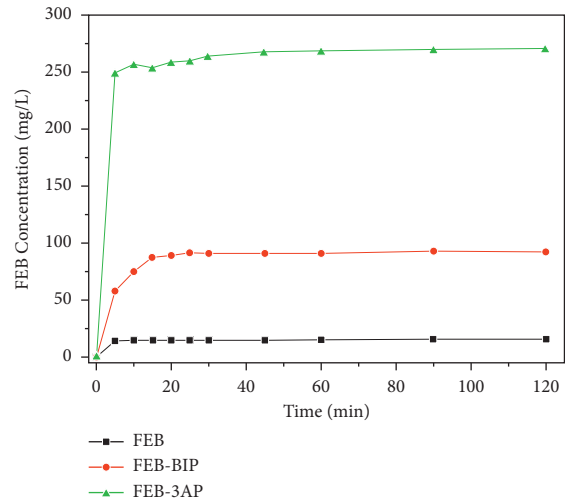

Figure 11: Powder dissolution profiles of FEB, FEB-BIP, and FEB-3AP at different time points in pure water at 37°C.

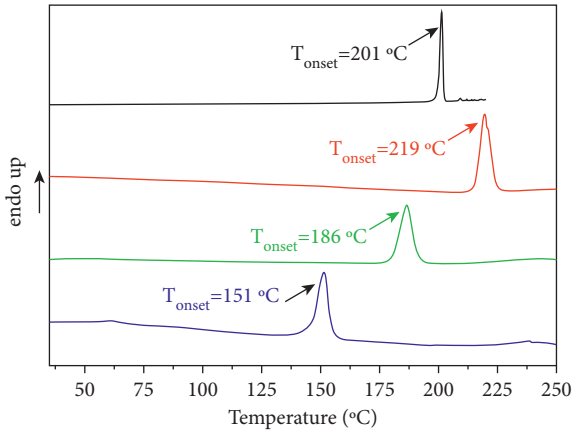

Figure 10: DSC curves of FEB (black), FEB-BIP cocrystal (red), FEB-3AP salt (green), and FEB-4HP-H2O salt (blue) recorded at 10°C /min heating rate.

FEB, FEB-BIP, and FEB-3AP were stable in water (Supplementary Materials, Figures S6–S8), while FEB-4HP-H_2O was unstable and underwent a phase change (Supplementary Materials, Figure S9). Both FEB-BIP and FEB-3AP were more soluble than FEB. The solubility of FEB-BIP and FEB-3AP was 5.15 and 15.19 times higher than that of pure FEB (17.7 mg L^{-1}). As expected, cocrystals and salts offered a remarkably increased release rate compared with pure FEB (Figure 11). The solubility and powder dissolution results indicated that cocrystallization significantly improved the solubility and release rate of FEB.

4. Conclusions

In this study, one new cocrystal and two salts of febuxostat, an antigout drug, with pyridine derivatives were synthesized using a solvent evaporation method. They were characterized by single-crystal X-ray diffraction, PXRD, and DSC techniques. The solubilities of FEB-BIP and FEB-3AP were 5.15 and 15.19 times higher than that of pure FEB. Compared with FEB, FEB-BIP cocrystal and FEB-3AP salt exhibited better dissolution and release rates. Such results suggested both BIP and 3AP were potential coformers in regulating the dissolution properties of febuxostat.

Data Availability

CCDC 2002500, 20099438, and 20099439 contain the supplementary crystallographic data for this study. These data can be obtained free of charge from The Cambridge Crystallographic Data Centre via https://www.ccdc.cam.ac.uk/structures.

Conflicts of Interest

The authors declare that they have no conflicts of interest.

Acknowledgments

The work was supported by the Guangxi Natural Science Foundation (2018GXNSFBA281167), the Basic Ability Promotion Project of Middle-Aged and Young Teachers in Colleges and Universities in Guangxi (2019KY0700), and the Wuzhou University Foundation (2020B006) for financial support of this research.

Supplementary Materials

Figure S1: library of coformers. Figure S2: The Fourier maps of FEB-4HP-H_2O salt. Figure S3: PXRD patterns for experimental (black) and simulated (red) of FEB-BIP cocrystal. Figure S4: PXRD patterns for experimental (black) and simulated (red) of FEB-3AP salt. Figure S5: PXRD patterns for experimental (black) and simulated (red) of FEB-4HP-H_2O salt. Figure S6: PXRD analysis of the residual materials of FEB after 24 h solubility in water. Figure S7: PXRD analysis of the residual materials of FEB-BIP cocrystal after 24 h solubility in water. Figure S8: PXRD analysis of the residual materials of FEB-3AP salt after 24 h solubility in water. Figure S9: PXRD analysis of the residual materials of FEB-4HP-H_2O salt after 24 h solubility in water. Table S1: The ΔpKa values of FEB and coformers used in this study. Table S2: the UV standard curves and concentration ranges of FEB, FEB-BIP, FEB-3AP, and FEB-4HP-H_2O. Table S3: powder solubility test results ($n = 3$). (*Supplementary Materials*)

References

[1] G. R. Desiraju, *Crystal Engineering: The Design of Organic Solids*, Elesevier, Amsterdam, Netherlands, 1989.

[2] G. R. Desiraju and T. Steiner, *The Weak Hydrogen Bond in Structural Chemistry and Biology; IUCr Monographs in Crystallography*, International Union of Crystallography, Chester, UK, 1999.

[3] P. Cerreia Vioglio, M. R. Chierotti, and R. Gobetto, "Pharmaceutical aspects of salt and cocrystal forms of APIs and characterization challenges," *Advanced Drug Delivery Reviews*, vol. 117, pp. 86–110, 2017.

[4] G. Kuminek, K. L. Cavanagh, M. F. M. da Piedade, and N. Rodríguez-Hornedo, "Posaconazole cocrystal with superior solubility and dissolution behavior," *Crystal Growth & Design*, vol. 19, no. 11, pp. 6592–6602, 2019.

[5] I. Kola and J. Landis, "Can the pharmaceutical industry reduce attrition rates?" *Nature Reviews Drug Discovery*, vol. 3, no. 8, pp. 711–716, 2004.

[6] S. Mittapalli, M. K. C. Mannava, U. B. R. Khandavilli, S. Allu, and A. Nangia, "Soluble salts and cocrystals of clotrimazole," *Crystal Growth & Design*, vol. 15, no. 5, pp. 2493–2504, 2015.

[7] L. Rajput, "Stable crystalline salts of haloperidol: a highly water-soluble mesylate salt," *Crystal Growth & Design*, vol. 14, no. 10, pp. 5196–5205, 2014.

[8] Y.-X. Zhang, L.-Y. Wang, J.-K. Dai et al., "The comparative study of cocrystal/salt in simultaneously improving solubility and permeability of acetazolamide," *Journal of Molecular Structure*, vol. 1184, pp. 225–232, 2019.

[9] K. Suresh and A. Nangia, "Lornoxicam salts: crystal structures, conformations, and solubility," *Crystal Growth & Design*, vol. 14, no. 6, pp. 2945–2953, 2014.

[10] M. K. C. Mannava, A. Gunnam, A. Lodagekar, N. R. Shastri, A. K. Nangia, and K. A. Solomon, "Enhanced solubility, permeability, and tabletability of nicorandil by salt and cocrystal formation," *CrystEngComm*, vol. 23, no. 1, pp. 227–237, 2021.

[11] P. Sanphui, G. Bolla, A. Nangia, and V. Chernyshev, "Acemetacin cocrystals and salts: structure solution from powder X-ray data and form selection of the piperazine salt," *IUCrJ*, vol. 1, no. 2, pp. 136–150, 2014.

[12] D. Maddileti, S. K. Jayabun, and A. Nangia, "Soluble cocrystals of the xanthine oxidase inhibitor febuxostat," *Crystal Growth & Design*, vol. 13, no. 7, pp. 3188–3196, 2013.

[13] D. P. Elder, R. Holm, and H. L. d. Diego, "Use of pharmaceutical salts and cocrystals to address the issue of poor solubility," *International Journal of Pharmaceutics*, vol. 453, no. 1, pp. 88–100, 2013.

[14] J. Wang, X.-L. Dai, T.-B. Lu, and J.-M. Chen, "Temozolomide-hesperetin drug-drug cocrystal with optimized performance in stability, dissolution, and tabletability," *Crystal Growth & Design*, vol. 21, no. 2, pp. 838–846, 2021.

[15] M. Pudipeddi, A. T. M. Serajuddin, D. J. W. Grant, and P. H. Stahl, "Solubility and dissolution of weak acids, bases, and salts," in *Handbook of Pharmaceutical Salts, Properties, Selection and Use*, P. H. Stahl and C. G. Wermuth, Eds., pp. 19–40, Wiley VCH, Weinheim, Germany, 2002.

[16] M. A. Becker, H. R. Schumacher Jr., R. L. Wortmann et al., "Febuxostat compared with allopurinol in patients with hyperuricemia and gout," *New England Journal of Medicine*, vol. 353, no. 23, pp. 2450–2461, 2005.

[17] K. Okamoto, B. T. Eger, T. Nishino, S. Kondo, E. F. Pai, and T. Nishino, "An extremely potent inhibitor of xanthine oxidoreductase," *Journal of Biological Chemistry*, vol. 278, no. 3, pp. 1848–1855, 2003.

[18] R. Khosravan, B. Gabowski, J. T. Wu, N. Joseph-Ridge, and L. Vernillet, *The Journal of Clinical Pharmacology*, vol. 65, pp. 355–363, 2007.

[19] J.-H. An, C. Lim, H. Ryu et al., "Structural characterization of febuxostat/l-pyroglutamic acid cocrystal using solid-state 13C-nmr and investigational study of its water solubility," *Crystals*, vol. 7, no. 12, p. 365, 2017.

[20] Y. Kang, J. Gu, and X. Hu, "Syntheses, structure characterization and dissolution of two novel cocrystals of febuxostat," *Journal of Molecular Structure*, vol. 1130, pp. 480–486, 2017.

[21] L.-Y. Li, R.-K. Du, Y.-L. Du et al., "Febuxostat-minoxidil salt solvates: crystal structures, characterization, interconversion and solubility performance," *Crystals*, vol. 8, no. 2, p. 85, 2018.

[22] X.-R. Zhang and L. Zhang, "Simultaneous enhancements of solubility and dissolution rate of poorly water-soluble febuxostat via salts," *Journal of Molecular Structure*, vol. 1137, pp. 328–334, 2017.

[23] L. Gao, X.-R. Zhang, Y.-F. Chen, Z.-L. Liao, Y.-Q. Wang, and X.-Y. Zou, "A new febuxostat imidazolium salt hydrate: synthesis, crystal structure, solubility, and dissolution study," *Journal of Molecular Structure*, vol. 1176, pp. 633–640, 2019.

[24] S. Modani, A. Gunnam, B. Yadav, A. K. Nangia, and N. R. Shastri, "Generation and evaluation of pharmacologically relevant drug-drug cocrystal for gout therapy," *Crystal Growth & Design*, vol. 20, no. 6, pp. 3577–3583, 2020.

[25] S. K. Rai, A. Gunnam, M. K. C. Mannava, and A. K. Nangia, "Improving the dissolution rate of the anticancer drug dabrafenib," *Crystal Growth & Design*, vol. 20, no. 2, pp. 1035–1046, 2020.

[26] Y.-n. Zhang, Y.-l. Liu, L.-x. Liu et al., "Tetrahydroberberine pharmaceutical salts/cocrystals with dicarboxylic acids: charge-assisted hydrogen bond recognitions and solubility regulation," *Journal of Molecular Structure*, vol. 1197, pp. 377–385, 2019.

[27] G. M. Sheldrick, *SHELXL-97*, University of Gottingen, Gottingen, Germany, 1997.